Turkish J. Eng. Env. Sci.
33 (2009) , 45 – 59.

doi:10.3906/muh-0901-6

# Moment redistribution and ductility of RHSC continuous beams strengthened with CFRP

**A. A. MAGHSOUDI**[1], **H. Akbarzadeh BENGAR**[2]
[1] *Civil Engineering Department, Kerman University, Kerman-IRAN*
*e-mail: Maghsoudi.a.a@mail.uk.ac.ir*
[2] *Civil Engineering Department, Kerman University, Kerman-IRAN*
*e-mail: h_akbarzadeh_b@yahoo.com*

Received 12.01.2009

**Abstract**

In continuous concrete beams, ductility allows redistribution of moment between the negative and positive moment zones. Although many in situ reinforced high strength concrete (RHSC) beams are of continuous construction, there has been very little research on such beams with external reinforcement. Due to premature debonding failures and the linear stress-strain characteristics of fiber reinforced polymer (FRP) up to failure, the ductility of plated members and their ability to redistribute moment is less than that of unplated RC beams.

The present study examined the responses of RHSC continuous beams, in terms of enhancement of moment and load capacity, moment redistribution, and different types of ductility. Thickness of carbon FRP (CFRP) sheets, strengthening of both the hogging and sagging region, and end anchorage technique were the main parameters investigated.

Various monitoring devices were used to monitor the loading history of the beams. Increasing the number of CFRP sheet layers increased ultimate strength, and decreased ductility, moment redistribution, and ultimate strain on CFRP sheets. Additionally, using end anchorage increased ultimate strength and moment redistribution. The moment enhancement ratio of the strengthened beams was significantly higher than the ultimate load enhancement ratio in the same beam. The proposed equation for converting the energy ductility index to the displacement ductility index provided accurate results.

**Key Words:** RHSC continuous beam; CFRP; End anchorage; Moment redistribution; Ductility.

## Introduction

Concrete structures can become deficient during their service life and require strengthening and repair. While many methods of strengthening structures are available, strengthening structures via external bonding of advanced fiber-reinforced polymer (FRP) composite has become very popular worldwide during the past decade due to the well-known advantages of FRP composites over other materials. Consequently, a great quantity of research, both experimental and theoretical, has been conducted on the behavior of FRP-strengthened reinforced

concrete (RC) structures, including beams, slabs, and columns (Meier et al., 1993; Teng et al., 2002). In this regard, the evolving technology of using carbon-bonded fiber-reinforced polymers (CFRP) for strengthening simply supported RC beams has attracted much attention in recent years. Fiber-reinforced polymer (FRP) materials in such forms as pultruded plates, fabrics, and sheets have been used as strengthening materials for RC beams. In particular, their practical implementations for flexural strengthening are numerous (Saadatmanesh and Ehsani, 1991; Arduini and Nanni, 1997; Spadea et al., 2001; Bencardino et al., 2002; Rabinovitch and Frostig, 2003; Toutanji et al., 2006; Camata, 2007; Li et al., 2008; Wang and Hsu, 2008), resulting in tremendous improvement in their application.

Possible failure mechanisms observed in experimental tests were reported by Teng et al. (2002). Premature failures, such as delamination, and FRP and laminate separation, can significantly limit capacity enhancement and the ultimate flexural capacity of the retrofitted beams.

Several studies were conducted to identify methods of preventing premature failure with the aim of improving the load capacity and ductility of RC beams. Researchers studied the use of end anchorage techniques, such as U-straps, L-shape jackets, and steel clamps, for preventing premature failure of RC beams strengthened with FRP sheets (Spadea et al., 1998; Pham Al-Mahaidi, 2006; Xiong et al., 2007).

Ductility is an important factor for any structural element or structure, especially in regions of seismic activity. Although external strengthening of RC beams with epoxy-bonded FRP has been established as an effective tool for increasing flexural and/or shear strength, the method still suffers from some drawbacks. Many of these drawbacks are attributed to the characteristics of currently available commercial CFRP strengthening systems. Although CFRPs have high strength, they are very brittle. When loaded in tension, FRPs exhibit a linear stress-strain behavior up to failure, without exhibiting a yield plateau or any indication of an impending failure. As FRPs behave differently than steel, they consequently suffer from a significant loss in beam ductility, particularity when CFRPs are used for flexural strengthening of RC beams (Saadatmanesh and Ehsani, 1991; Arduini and Nanni, 1997; Spadea et al., 2001; Bencardino et al., 2002; Toutanji et al., 2006).

With recent advancements in concrete technology, and the availability of various types of mineral and chemical admixtures and very powerful superplasticizers, concrete with a compressive strength of up to 100 MPa can now be produced commercially with an acceptable level of variability using ordinary aggregates. These developments have led to increased applications of high-strength concrete (HSC) all around the globe. Although HSC offers many advantages over conventional concrete, as the strength of concrete increases some of its characteristics and engineering properties become different from those of normal-strength concrete (NSC) (ACI, 1992; Rashid et al., 2002). These differences in material properties may have important consequences in terms of the structural behavior and design of HSC members (Oztekin et al., 2003). This concrete, with very high compressive strength, can result in less ductile responses of the structural members. It has been determined that flexural ductility, in terms of maximum curvatures attainable, may be less in HSC beams (Rashid et al., 2002).

HSC provides a better solution for reducing the size and weight of concrete structural elements, particularly for long-span beams (Ashour, 2000). HSC structures can become deficient during their service life and require strengthening and repair. This need may arise as a result of design or construction errors, functional changes, changes in design codes, or damage accumulated over time or caused by accidental overloading, fires, or earthquakes. While complete replacement of a deficient/deteriorated structure is an option, strengthening/repair is often a more economical option.

Although many in situ RC beams are of continuous construction, there has been very little research into the behavior of such beams with external reinforcement (El-Refaie et al., 2003a; Ashour et al., 2004; Grace et al., 2004). In addition, most design guidelines have been developed for simply supported beams with external FRP laminates (FIB, 2001; JSCE, 2001; ACI, 2002). Ductility is even more important for statically indeterminate structures, such as continuous beams, as it allows for moment redistribution through the rotation of plastic hinges. Moment redistribution facilitates utilization of the full capacity of more segments of the beam.

Ashour et al. (2004) reported that all strengthened beams have increased beam load capacity, but lower ductility than their respective non-strengthened control beams, and that increasing CFRP sheet length to cover the entire hogging or sagging zone did not prevent premature failure. Further research on the performance of end anchorage techniques is necessary to minimize the risk of this type of failure; strengthening the top surface at the central support and the beam soffit was reported to be the most effective configuration for CFRP laminates for enhancing beam load capacity (El-Refaie et al., 2003a; Ashour et al., 2004).

Grace et al. (2004) investigated the effectiveness of a new triaxially braided ductile fabric in providing ductility in RC continuous beams strengthened in flexure. As previously mentioned, ductility is an important factor in the design of HSC members under flexure; therefore, the present study examined the use of RHSC continuous beams strengthened with CFRP. The objective of this research was to examine the ultimate stage and ductility of RHSC continuous beams in structures strengthened with CFRP sheets. The experiment included 5 continuous (2-span) beams with overall dimensions equal to 250 × 150 × 6000 mm. Each beam was loaded with a concentrated load at the middle of the span. Thickness of CFRP sheets, strengthening of both the hogging and sagging regions, and end anchorage technique were the main parameters investigated. During the experiment, deflection and strains on concrete compressive regions, and along the CFRP sheets at the central support and mid span were measured until failure. The responses of the continuous beams were examined and are discussed in terms of moment and load capacity, moment redistribution, and different types of ductility.

## Experiment

### Test specimens and CFRP bonding procedure

Five large-scale RC 2-span beams were tested until failure: 1 HSRC control beam and 4 HSRC beams strengthened with externally bonded CFRP sheets on the tension face. Beam geometry and reinforcement, as well as loading and support configurations are illustrated in Figure 1. The beams were symmetrically reinforced with two 16-mm diameter rods at the top and bottom. To avoid shear failure, the beams were slightly over-designed for shear, with 10-mm diameter closed stirrups spaced every 100 mm.

Thickness of CFRP laminates and end anchorage were the main parameters investigated, as summarized in Table 1. Thickness and width of each layer of CFRP sheet were 0.11 mm and 145 mm, respectively. The control beam (CB) had no external reinforcement. The other beams were strengthened at both negative and positive moment regions. The SC1 beam employed 1 layer of CFRP sheet, while the SC2 and SC3 beams used 2 and 3 layers of CFRP sheet, respectively, with U-wrap at the ends of the laminates. The SC3N beam used 3 layers of CFRP sheet, without end straps. SC3N was prepared in order to understand the effectiveness of end anchorage on the ductility and flexural strength of RHSC continuous beams. The end anchorage system, consisting of 2 or 3 plies of CFRP sheet 150 mm wide, was wrapped and bonded around the sides and the soffit of the concrete beams near the end of the longitudinal CFRP sheets (Figure 1).

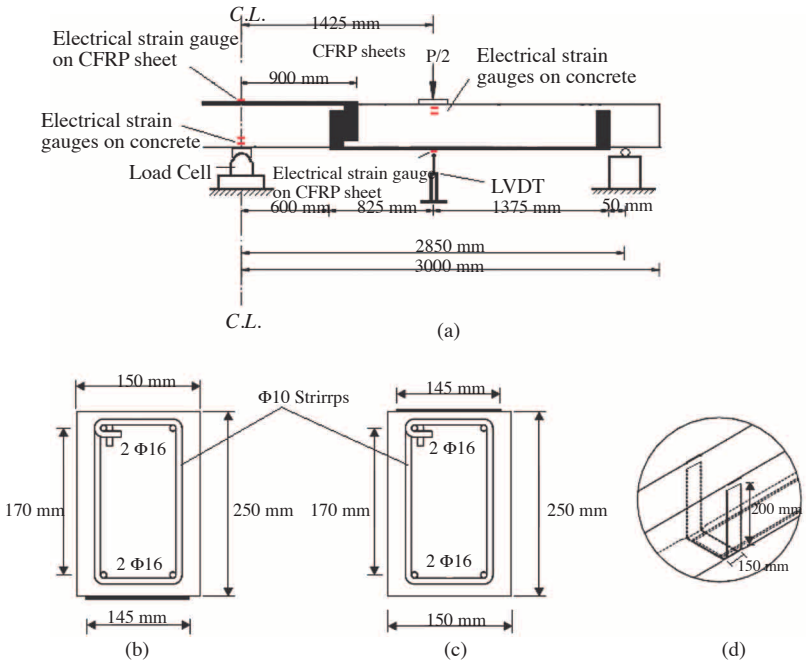


**Figure 1.** Test set-up and monitoring devices. (a) Longitudinal profile of beam, (b) typical cross section of beam in sagging region, (c) ) typical cross section of beam in hogging region, and (d) end anchorage system.

**Table 1.** Details of the test beams.

| Beam no. | *f'c* (MPa) | Positive moment strengthening | | Negative moment strengthening | | End anchorage |
|---|---|---|---|---|---|---|
| | | No. of layers CFRP sheets | Strengthened Length (m) | No. of layers CFRP sheets | Strengthened Length (m) | |
| CB | 74.2 | 0 | 2.20 | 0 | 1.8 | None |
| SC1 | 74.6 | 1 | | 1 | | None |
| SC2 | 74.1 | 2 | | 2 | | Yes |
| SC3N | 75.6 | 3 | | 3 | | None |
| SC3 | 74.4 | 3 | | 3 | | Yes |

The process of applying the CFRP sheets to concrete involved surface preparation, priming, resin undercoating, CFRP sheet application, and resin overcoating. Prior to bonding the CFRP sheets, the beams were ground using a mechanical grinder in order to obtain a clean sound surface free of all contaminants and then cleaned with an acetone solution. After that, a 2-part primer was applied to the prepared concrete surface. Next, a 2-part epoxy resin was applied to the primed concrete surface, followed by application of the CFRP sheet. Finally, a resin overcoat was applied over the CFRP sheet. Concrete beams strengthened with CFRP sheets were cured for at least 7 days at room temperature before testing.

### Material Properties

The HSC mix was designed by the first author and its mix proportions, with the maximum size of coarse aggregate (10 mm), are given in Table 2. For each beam six 100 × 100 × 100-mm concrete cubes were made at the time of casting and were kept with the beams during curing. Mean concrete compressive strength ($f'_c$) for each beam is shown in Table 1. The relationship between cylinder strength ($f'_c$) and cube strength was ($f'c$= 0.85 $f_{cu}$).

Two 16-mm diameter bars (Φ16) were tensile tested; the measured yield strength was 412.5 MPa and maximum tensile strength was 626.4 MPa. The modulus of elasticity of the steel bars was 2 × $10^5$ MPa.

Young's modulus ($E_{fu}$) and ultimate tensile stress ($f_{fu}$) of the CFRP sheets, and the properties of the epoxies used for bonding the CFRP sheets were obtained from the supplier and are given in Tables 3 and 4.

**Table 2.** Concrete mixture proportions.

| Cement (kg/m$^3$) | Silica fume (kg/m$^3$) | Coarse agg. (kg/m$^3$) | Fine agg. (kg/m$^3$) | Super lasticizer (kg/m$^3$) | W/C ratio |
|---|---|---|---|---|---|
| 650 | 55 | 723 | 645 | 11.7 | 0.32 |

**Table 3.** Mechanical properties of the CFRP sheets.

| Material | Density (kg/cm$^3$) | Thickness (mm) | Ultimate Tensile stress $f_{fu}$ (MPa) | Young's Modulus $E_{fu}$ (GPa) | Ultimate strain $\varepsilon_{fu}$(%) |
|---|---|---|---|---|---|
| CFRP | 1.81 | 0.11 | 3800 | 242 | 1.55 |

**Table 4.** Mechanical properties of the bonding adhesive.

| Material | Density (kg/cm$^3$) | Compression strength (MPa) | Tensile strength (MPa) | Young's Modulus (GPa) | Shear strength (MPa) |
|---|---|---|---|---|---|
| Epoxy resin adhesive | 1.11 | 97.4 | 76.1 | 3.6 | 54.8 |
| Epoxy resin primer | 1.77 | >90 | >25 | 12.8 | >15 |

### Instrumentation and test procedure

Each test beam comprised of 2 equal spans of 2850 mm was loaded with a concentrated load at the middle of the span (Figure 1). The various monitoring devices and their locations along the beam appear in Figure 1. A hydraulic actuator was used to load the beam. The reaction of the beam at the central support was measured using a load cell. Disposable electrical resistance strain gauges were pasted on tensile bars and on the CFRP sheets at specific locations (Figure 1) to monitor the development of CFRP strain throughout the loading history. The electrical gauges were also attached along the height of the beams at the midspans and the central support to measure concrete compressive strain. Midspan deflections were measured using linear

variable differential transformers (LVDTs). The load was applied step-by-step up to failure in a load-control manner. Strain gauge, LVDT, and the load cell readings were recorded at each load increment using data logging equipment. At the end of each load increment, observations, measurements, crack development, and propagation on the beam surfaces were recorded.

### Test Results and Discussion

All beams were loaded with a concentrated load at the middle of the span. The obtained experimental results are presented and subsequently discussed in terms of the observed mode of failure, enhancement of load and moment capacity, moment retribution, and different types of ductility.

### Failure mode and ultimate strain

The cracking patterns and failure modes for various test beams are shown in Figures 2-6. Three different failure modes were observed (Table 5) and are described.

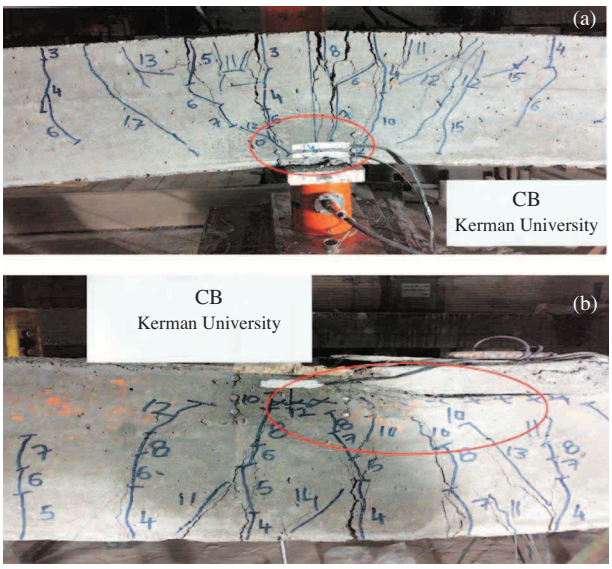


**Figure 2.** Conventional ductile failure of the CB. (a) Concrete crushing at the central support and (b) concrete crushing at mid-span.

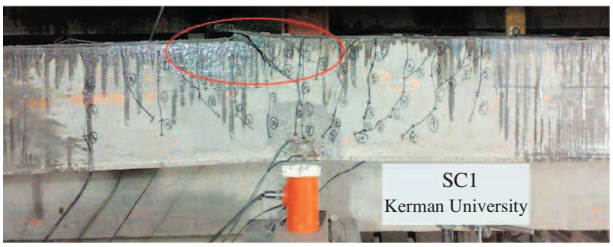


**Figure 3.** Rupture of FRP at the central support in SC1.

The CB (without strengthening plates) was designed to fail in flexure. Failure of the CB was due to concrete-induced crushing in the compression zone of both the central support ($P_u$ = 162.0 kN) and midspan section after tension steel yielded ($P_y$ = 105.0 kN, see later in Figure 7a), as shown in Figure 2.

At the central support of SC1 the tension steel yielded ($P_y$ = 110.0 kN, see later in Figure 7a) and the beam failed ($P_u$ = 190.6 kN) due to tensile rupture of the CFRP sheet over the central support (Figure 3). Rupture of the CFRP sheets was sudden and accompanied by a loud noise, indicating a rapid release of energy and a total loss of load capacity.

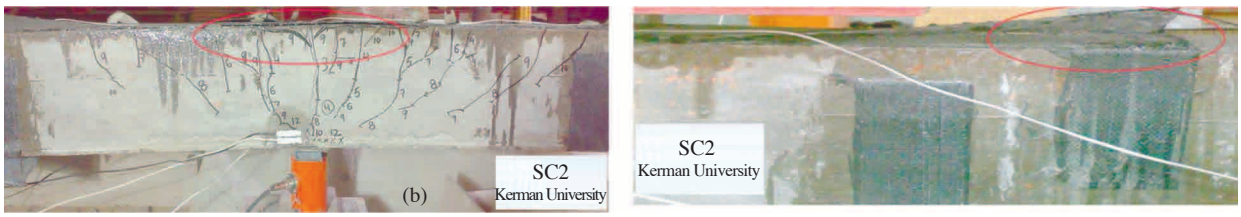


(a) (b)

**Figure 4.** Failure modes observed in SC2. (a) IC debonding at the negative moment and (b) rupture of the end strap at the hogging region.

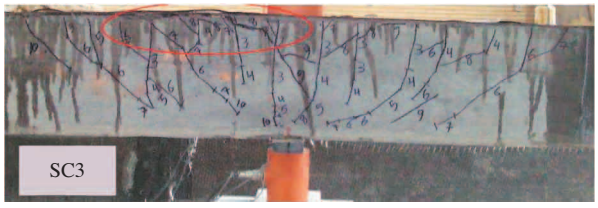


**Figure 5.** IC debonding at negative moment in SC3 beam.

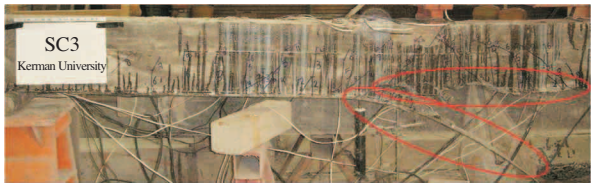


**Figure 6.** IC debonding at the positive moment in SC3N.

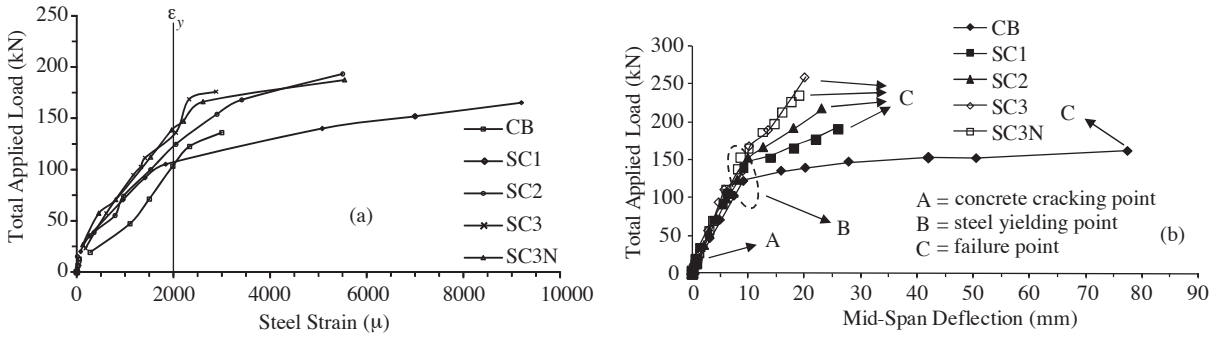


**Figure 7.** Total applied load versus (a) tensile steel strain at the central support and (b) midspan deflection curves of the tested beams.

At the central support of SC2 the tension steel yielded ($P_y = 124.6$ kN, see later in Figure 7a) and the beam exceeded the load achieved by SC2 and failed suddenly at a load of $P_u = 193.3$ kN due to intermediate crack (IC) debonding at the negative moment strengthening CFRP sheet, as shown in Figure 4, followed by rupture of the end strap at the hogging region and (IC) debonding at the positive moment strengthening CFRP sheet ($P_u = 219.3$ kN).

Based on experimental observation, the debonding failure can be explained as follows: due to the flexural cracks formed in the central support as the load increased, the bond between the FRP and concrete started to fracture at a certain load level and the failure propagated towards the mid-span until most of the FRP composites detached from the concrete beams. It can be seen that the bond between the FRP and concrete was not strong enough to ensure the rupture of the composites with more than 1 layer of carbon fiber sheets; thus, the FRP-concrete bond strength controlled the failure mode when more than 1 layer of fiber sheets were bonded. When 1 layer of carbon fiber is applied, the bond problem is not a factor controlling failure; thus, the force in the FRP will reach its ultimate tensile capacity when the beam fails.

**Table 5.** Beam test results, including ultimate and yielding of load, and deflection and ultimate strain of CFRP.

| Beam no. | Failure mode | $P_y$ (kN) | $\xi$ | $P_u$ (kN) | $\lambda$ | Compressive concrete ultimate strain (micron) | | Ultimate strain of CFRP (micron) | |
|---|---|---|---|---|---|---|---|---|---|
| | | | | | | Central support | Midspan | Central support | Midspan |
| CB | Flexural failure | 105 | 1 | 162 | 1 | 4400 | 4600 | - | - |
| SC1 | Rupture of top CFRP sheet at hogging region | 110 | 1.05 | 190.6 | 1.18 | 1800 | 2500 | 10000 | 10618 |
| SC2 | IC debonding at hogging region followed by rupture of end strap at hogging region | 124.6 | 1.18 | 219.3 | 1.35 | 2700 | 2800 | 7030 | 7785 |
| SC3 | IC debonding at hogging region | 136 | 1.29 | 259.3 | 1.6 | 2600 | 2600 | 8922 | 7000 |
| SC3N | IC debonding at sagging region | 138.6 | 1.32 | 236 | 1.45 | 2100 | 1900 | 6704 | 7268 |

At the central support of SC3 the tension steel yielded ($P_y$= 136.0 kN, see later in Figure 7a) and the beam failed via IC debonding at the negative moment (Figure 5). End straps did not rupture because 3 layers of U-wrap were used.

At the central support of SC3N the tension steel yielded ($P_y$= 138.6 kN, see later in Figure 7a) and the beam failed ($P_u$= 236.0 kN) via IC debonding at the positive moment (Figure 6).

For the tested beams concrete was not initially pre-cracked and the development of the cracks during the test was greatly influenced by the number of CFRP layers. The occurrence of the first crack was delayed and more diffuse. Shear cracks occurred in the beams for an applied load of about 70% of the ultimate load. Figures 3-6 also indicate that the strengthened beams had many diagonal cracks, which were caused by the increase in flexural capacity due to the CFRP sheets.

The maximum recorded strain values for the CFRP sheets and compressive concrete at the central support and mid span before beam failure load are given in Table 5. It can be seen that increasing the number of CFRP layers in strengthened beams reduced the tensile ultimate strain of the CFRP sheets. Moreover, use of end anchorage in the strengthened beams increased the failure strain of CFRP sheets. Strengthening beams significantly reduced the ultimate concrete compressive strain.

**Load-Deflection and Enhancement of Failure Load**

The total applied load versus tensile steel strain at the central support and deflection diagrams at mid-span of tested beams are shown in Figure 7. Figure 7b indicates that each strengthened continuous beam curve exhibited almost 3 straight lines with slightly different responses up to failure, representing the concrete pre-cracking (OA), concrete post-cracking tension steel pre-yield (AB), and tension steel post-yield stages (BC). Yet, the CB showed almost 2 straight lines of pre-cracking and post-cracking behavior, with a yield plateau in the post-yield stage.

Behavior of the beams was very similar in the uncracked elastic stage. In other words, the beams' flexural stiffness was the same until the occurrence of cracks in the concrete. In the cracked pre-yield stage (Figure 7b) the stiffness of the strengthened beams was slightly higher than that of the CB; however, significant decreases in beam stiffness were observed after yielding of tensile steel at the negative and positive moment sections, whereas by increasing the number of CFRP layers the loss of beam stiffness was reduced. Increasing the number of CFRP layers decreased midspan deflection and generally increased stiffness for the same value of applied load. Comparing SC3 and SC3N, it was observed that using end anchorage can slightly increase beam stiffness after yielding of tensile steel.

Table 5 summarizes the ultimate failure load, $P_u$ (the sum of the 2 mid-span point loads at failure), ultimate load enhancement ratio ($\lambda$), which is the ratio of the ultimate load of an externally strengthened beam to the CB, yielding load of tension steel at the central support ($P_y$), and yielding load enhancement ratio ($\xi$), which is the ratio of the yielding load of the strengthened beam to that of the CB. As indicated in Table 5, addition of 1, 2, and 3 layers of CFRP sheet increased the ultimate load capacity by 18%, 35%, 60%, and 45% for SC1, SC2, SC3, and SC3N, respectively, in comparison to the CB. Use of end straps led to increased load capacity of the strengthened beam, based on comparison of the results for SC3 and SC3N. Additionally, by increasing the number of CFRP layers, the yielding load of tension steel increased slightly at the central support. The use of end straps did not increase the yielding load.

**Enhancement of moment capacity and moment redistribution**

Table 6 presents the failure moments and the ultimate moment enhancement ratio ($\chi$, which is the ratio of the ultimate moment of strengthened sections (central support and midspan sections) to that of the non-strengthened sections. Beam bending moment was calculated from the equilibrium considerations, using the measured central support reaction and mid-span applied load. The results shown in Table 6 indicate that the addition of 1, 2, and 3 layers of CFRP sheet increased the ultimate moment capacity at the central support by 28%, 55%, 88%, and 73%, and at midspan by 12%, 26%, 47%, and 33%, for SC1, SC2, SC3, and SC3N, respectively, as compared to the CB. It was possible to increase the moment capacity of the strengthened beams at the hogging and sagging regions by using end U-straps (see the results of SC3 and SC3N). In general, all the strengthened sections resisted a higher moment than the corresponding unstrengthened sections of the CB. Comparing the ultimate load enhancement ratio of a strengthened beam and the moment enhancement ratio of a strengthened section at the central support of the same beam, it can be concluded that the latter was significantly higher than the former (a similar conclusion was reported by Ashour et al. (2004) and El-Refaie et al. (2003)); however, this is not the case for simply supported beams strengthened with external reinforcement for which the moment and load enhancement ratios are always the same (Hashemi et al., 2008).

The moment redistribution ratio ($\beta$ given in Table 6 was calculated for the sagging and hogging bending moments at midspan and at the central support, respectively, for beam failure load using Eq. (1):

**Table 6.** Central support reaction, failure moment, and moment redistribution of the tested beams.

| Beam NO. | $P_u$ (kN) | Central support Reaction (R ) (kN) | Central support | | | | mid span | | | |
|---|---|---|---|---|---|---|---|---|---|---|
| | | | failure moment (kNm) | χ | failure moment based on elastic analysis (kN.m) | β (%) | failure moment (kNm) | χ | failure moment based on elastic analysis (kN.m) | β (%) |
| CB | 162.0 | 106.5 | 36.33 | 1.00 | 43.28 | 16.06 | 39.54 | 1.00 | 36.07 | -9.62 |
| SC1 | 190.6 | 128.1 | 46.74 | 1.28 | 50.93 | 8.22 | 44.53 | 1.12 | 42.44 | -4.92 |
| SC2 | 219.3 | 149.3 | 56.50 | 1.55 | 58.59 | 3.57 | 49.87 | 1.26 | 48.83 | -2.13 |
| SC3 | 259.3 | 177.4 | 68.26 | 1.88 | 69.28 | 1.51 | 58.14 | 1.47 | 57.73 | -0.71 |
| SC3N | 236.0 | 162 | 62.7 | 1.73 | 63.06 | 0.57 | 52.72 | 1.33 | 52.54 | -0.34 |

$$\beta = \frac{M_e - M_E}{M_e} \times 100\% \tag{1}$$

where $M_e$ is the value of the failure moment at the central support and midspan based on the known elastic analysis, and$M_E$ is the experimental bending moment value. As shown in Table 6, the CB had a moment redistribution ratio of 16.06 at the central support and -9.62 at midspan. The moment redistribution ratio of the strengthened beams significantly decreased as the number of CFRP layers increased. SC1, SC2, SC3, and SC3N had moment redistribution ratios of 8.22, 3.57, 1.51, and 0.57 at the central support and -4.92, -2.13, -0.71, and -0.34 at midspan, respectively. Yet, by comparing the results for SC3 and SC3N it was observed that use of end U-straps slightly increased the moment redistribution ratio.

## Ductility

Ductility is important for statically indeterminate structures, such as continuous beams, as it allows for moment redistribution through the rotation of plastic hinges. A ductile material is one that can undergo significant strain while resisting load. When applied to RC members, the term ductility implies the ability to sustain significant inelastic deformation prior to collapse. As the evolving technology of using bonded CFRP for strengthening RC beams has attracted much attention in recent years and because HSC behaves like a brittle material, understanding the effects of such materials on the ductility of RC beams is critical (Maghsoudi and Akbarzadeh, 2006; Hashemi et al., 2008).

Ductility has generally been measured by a ratio called the ductility index or factor ($\mu$). The ductility index is usually expressed as a ratio of rotation ($\theta$), curvature ($\phi$), deflection (displacement) ($\Delta$), and absorbed energy (E) at failure (peak load) divided by the corresponding property when the steel starts yielding. In the present study, ductility was obtained based on displacement and absorbed energy methods.

*Displacement ductility results and discussions* Figure 8 schematically shows the response of a strengthened RC beam. Point A corresponds to initial concrete cracking, point B to the first steel yielding, and point C to failure. Based on Figure 8, the displacement ductility index is defined by Eq. (2):

$$\mu_\Delta = \frac{\Delta_u}{\Delta_y} \tag{2}$$

where $\Delta_u$ is the midspan deflection at ultimate beam load and $\Delta_y$ is the midspan deflection at yielding load of the tensile steel reinforcement at the central support.

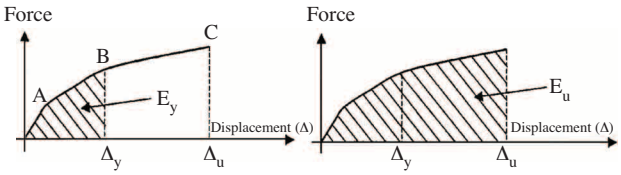


**Figure 8.** Definition of displacement and energy ductility (Thomsen et al., 2004).

Table 7 shows the experimental values of ($\Delta_u$), ($\Delta_y$), the displacement ductility index value of ($\mu_\Delta$), and percentage of decrease of displacement ductility in the CB. It can be seen that increasing the number of CFRP sheet layers led to decreased mid span deflection at ultimate load, while the midspan deflection at yielding load was almost constant. Therefore, increasing the number of CFRP sheet layers decreased the beam displacement ductility index.

**Table 7.** Comparison of displacement and absorbed energy of the tested beams.

| Beam no. | ($\Delta_u$) (mm) | ($\Delta_y$) (mm) | ($\mu_\Delta$) by Eq. (2) | Decrease over control beam (%) | ($E_y$) (kN.mm) | ($E_U$) (kN.mm) | ($\mu_E$) by Eq. (3) | Decrease over control beam (%) | ($\mu_{Ep}$) by Eq. (4) |
|---|---|---|---|---|---|---|---|---|---|
| CB | 7.5 | 77.4 | 10.32 | ---- | 415.2 | 10720 | 25.82 | ---- | 10.26 |
| SC1 | 7.5 | 26 | 3.47 | 66.4 | 496 | 3499 | 7.05 | 72.7 | 3.32 |
| SC2 | 8 | 23 | 2.87 | 72.2 | 539.24 | 3253.8 | 6.03 | 76.6 | 2.94 |
| SC3 | 8.9 | 19.88 | 2.23 | 78.4 | 723.17 | 2958.6 | 4.09 | 84.1 | 2.22 |
| SC3N | 8 | 19 | 2.37 | 77.0 | 602 | 2733 | 4.53 | 82.4 | 2.38 |

Figure 9 illustrates the effect of the quantity of CFRP on displacement ductility of RHSC continuous beams. For HSC members, a displacement ductility index ($\mu_\Delta$ in the range of 3-5 is considered imperative for adequate ductility, especially in areas of seismic design and the redistribution of moments (Ashour, 2000; Maghsoudi and Akbarzadeh, 2006). Therefore, assuming that an index value of 3 represents the minimum for ensuring the ductile behavior of RHSC continuous beams strengthened with CFRP sheet, it appears that the tested beams (SC2, SC3, and SC3N) with a CFRP sheet ratio ($A_f/(b \times h)$) greater than 0.051 would not meet that requirement ($A_f$is the FRP cross-sectional area, and $b$ and $h$ are width and height of beams, respectively).

*Energy-based method of ductility results and discussion* Another method of determining ductility is based on the energy definition; Thomsen et al. (2004) suggested an energy-based definition of ductility, which is illustrated in Figure 8. The energy ductility index ($\mu_E$) is defined as the ratio between the energy of the system at failure ($E_u$) and the energy of the system at yielding load of tensile steel reinforcement at the central support ($E_y$):

$$\mu_E = \frac{E_u}{E_y} \tag{3}$$

The failure energy at beam ultimate load ($E_u$), elastic energy at first steel yield load ($E_y$), the energy ductility index ($\mu_E$), and percentage of decrease of energy ductility of the CB is given in Table 7. Similar to the

displacement ductility index, increasing the number of CFRP sheet layers led to a decrease in the absorbed energy at failure load; consequently, the energy ductility index of strengthened beams decreased by 72.7%, 76.6%, 84.1%, and 82.4% for SC1, SC2, SC3, and SC3N, respectively, based on Eq. (3).

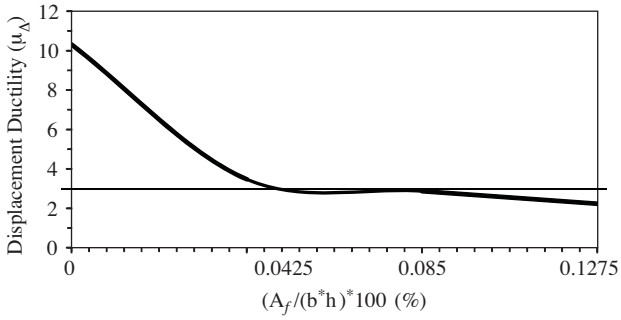


**Figure 9.** Effect of CFRP on displacement ductility.

Reinforced concrete structures usually behave in a ductile manner if an appropriate amount of steel reinforcement is added. Ductility is achieved by inelastic deformation of the steel before failure. During this period a concrete beam consumes much of the energy, causing the elastic energy released at failure to be reduced; however, the circumstance is not the same for RC beams strengthened with CFRP, because this material usually cannot attain inelastic deformation. This causes a tremendous amount of elastic strain energy to build up, which exceeds that of steel reinforcement, and can be released at failure.

As seen in Table 7, a comparison between energy and the displacement ductility ratio shows that for all the beams tested the energy ductility index value was about 2-fold higher than the displacement ductility index; however, while considering the energy ductility index ($\mu_E$)we observed that none of the index values represented an acceptable minimum energy ductility value for ensuring the ductile behavior of RHSC continuous beams strengthened with CFRP sheets. As such, for assimilating the amount of displacement and energy ductility it is possible to use the minimum value of the displacement ductility index (3) for the energy ductility index. Therefore, a new energy ductility index equation was proposed for assimilating the amount of displacement and energy ductility. The quantity of the proposed energy ductility index ($\mu_{Ep}$) is assumed by Eq. (4) and Table 7 lists the obtained values for the beams we tested. It is clear that the $\mu_{Ep}$ values are very close to the $\mu_\Delta$ values.

$$\mu_{Ep} = 0.37\frac{E_u}{E_y} + 0.71 \tag{4}$$

To assess further the accuracy of the proposed Eq. (4), the only available study on the energy ductility of RC continuous beams strengthened by CFRP was also considered, and the energy ductility index values for the test beams reported therein were calculated and are presented in Table 8 (El-Refaie et al., 2003b). The results listed in Table 8 demonstrate that, except for E2, the percentage of error obtained by the proposed equation for calculating the energy ductility of the test beams was less than 10%; therefore, the accuracy of the proposed equation is high.

**Table 8.** Deflection and proposed energy ductility ratio of the test beams reported by El-Refaie et al. (2003b).

| Beam no. | Deflection ductility ratio, ($\mu_\Delta$) by Eq. (2) | ($E_y$) (kN.mm) | ($E_u$) (kN.mm) | Energy ductility ratio, ($\mu_E$) by Eq. (3) | Proposed energy ductility ratio, ($\mu_{Ep}$) by Eq. (4) | Error of proposed equation (Eq.(2)-Eq.(4))/ Eq.(2)×100 |
|---|---|---|---|---|---|---|
| E2 | 2.48 | 1373.11 | 5286.50 | 3.85 | 2.13 | 14.11 |
| E3 | 3.21 | 831.18 | 5161.68 | 6.21 | 3.01 | 6.23 |
| E4 | 2.1 | 1328.49 | 4556.73 | 3.43 | 1.98 | 5.71 |
| E5 | 2.02 | 1399.2 | 4393.50 | 3.14 | 1.87 | 6.82 |

## Conclusions

The following conclusions can be drawn based on the RHSC continuous strengthened beam test results:

1- Increasing the number of CFRP sheet layers changed the failure mode from tensile rupture to IC debonding. End U-straps were effective in limiting end debonding, but not intermediate span debonding.

2- Increasing the number of CFRP layers reduced the tensile ultimate strain in the CFRP sheets. Use of end anchorage in strengthened continuous beams increased the tensile ultimate strain of CFRP sheets.

3- Load and moment capacity of the strengthened beams increased as the number of CFRP layers increased. Use of end straps led to increased load and moment capacity of the strengthened continuous beams.

4- The moment enhancement ratio at the central support of the strengthened continuous beams was significantly higher than the ultimate load enhancement ratio at the span of the same beams.

5- Increasing the number of CFRP layers significantly decreased the moment redistribution ratio from 16.06 to 1.51.

6- Assuming that an index value of 3 represents the acceptable minimum to ensure the displacement ductile behavior of RHSC continuous beams strengthened with CFRP sheets, the tested beams (SC2, SC3, and SC3N) with a CFRP sheet ratio ($Af/(b \times h)$) greater than 0.051 would not meet that requirement. In other words, displacement ductility decreased as the the number of CFRP sheet layers increased.

7- Similar to the displacement ductility index, increasing the number of CFRP sheet layers led to a decrease in the absorbed energy at failure load of the beams; consequently, the energy ductility index of the strengthened beams decreased by 72.7%, 76.6%, 84.1%, and 82.4% for SC1, SC2, SC3, and SC3N, respectively.

8- For all the beams tested, the energy ductility index was about 2-fold higher than the displacement ductility index value; therefore, a new energy ductility index equation was proposed for assimilating the amount of displacement and energy ductility. Using the proposed energy ductility index equation ($\mu_{Ep}$) it was possible to achieve almost the same results as when the displacement ductility index equation ($\mu_\Delta$ was used.

## Acknowledgments

The authors gratefully acknowledge the support of the Iran National Science Foundation (INSF).

## References

ACI, State-of-the-Art Report on High-Strength Concrete, ACI 363R, Detroit, 1992.

ACI, Guide for the Design and Construction of Externally Bonded FRP Systems for Strengthening Concrete Structures", Farmington Hills. Mich.: American Concrete Institute, ACI 440.2R-02, 2002.

Arduini, M. and Nanni, A., "Behaviour of Precracked RC Beams Strengthened with Carbon FRP Sheets", ASCE Journal of Composites for Construction, 1(2), 63-70, 1997.

Ashour, S.A. "Effect of compressive strength and tensile reinforcement ratio on flexural behavior of high-strength concrete beams", Engineering Structures 22, 413-423, 2000.

Ashour, A.F., El-Refaie, S.A. and Garrity, S.W., "Flexural Strengthening of RC Continuous Beams using CFRP Laminates", Cement & Concrete Composits, 26, 765-775, 2004.

Bencardino, F., Spadea, G. and Swamy, N., "Strength and Ductility of Reinforced Concrete Beams Externally Reinforced with Carbon Fiber Fabric." ACI Structural Journal, 99, 163-171, 2002.

Camata, G., Spacone, E. and Zarnic, R., "Experimental and Nonlinear Finite Element Studies of RC Beams Strengthened with FRP Plates", Composites: Part B, 38, 277-288, 2007.

El-Refaie, S.A., Ashour, A.F. and Garrity, S.W., "Sagging and Hogging Strengthening of Continuous Reinforced Concrete Beams using Carbon Fiber-reinforced Polymer Sheets", ACI Structural Journal, 100, 446-453, 2003a.

El-Refaie, S.A., Ashour A.F. and Garrity, S.W. "CFRP Strengthened Continuous Concrete Beams", Structures & Buildings, 156, Issue SB4, 395-404, 2003b.

FIB, "Externally Bonded FRP Reinforcement for RC Structures, Fe'de'ration Internacionale du beton, Task Group 9.3 FRP, 2001.

Grace, N.F., Ragheb, W.F. and Abdel-Sayed, G., "Strengthening of Cantilever and Continuous Beams using New Triaxially Braided Ductile Fabric." ACI Structural Journal, 101, 237-244, 2004.

Hashemi, H., Maghsoudi, A.A. and Rahgozar, R., "Flexural Ductility of Reinforced HSC Beams Strengthened with CFRP Sheets" Structural Engineering and Mechanic, 2008, (in press).

JSCE, Recommendations for the Upgrading of Concrete Structures with Use of Continuous Fiber Sheets", Tokyo: Japanese Society of Civil Engineers, Concrete engineering, Series 41, 2001.

Li, L., Guo, Y. and Liu, F., "Test Analysis for FRC Beams Strengthened with Externally Bonded FRP Sheets." Construction and Building Materials, 22, 315-323, 2008.

Maghsoudi, A.A. and Akbarzadeh, H., "Flexural Ductility of HSC Members", Structural Engineering and Mechanics, 24 (2), 2006.

Meier, U., Deuring, M., Meier, H. and Schwegler, G., Strengthening of Structures with Advanced Composites. Alternative materials for reinforcement and prestressing of concrete, Clarke/Chapman & Hall. Glasgow, Scotland: J.L., 1993.

Oztekin, E., Pul, S. and Husem, M., "Determination of Rectangular Stress Block Parameters for High Performance Concrete", Engineering Structures, 25, 371-376, 2003.

Pham, H. and Al-Mahaidi, R., "Prediction Models for Debonding Failure Loads of Carbon Fiber Reinforced Polymer Retrofitted Reinforced Concrete Beams", ASCE Journal of Composites for Construction, 10, 48-59, 2006.

Rabinovitch, O. and Frostig, Y., "Experiments and Analytical Comparison of RC Beams Strengthened with CFRP Composites", Composites: Part B, 34, 663-677, 2003.

Rashid, M.A., Mansur, M.A. and Paramasivam, P., "Correlations Between Mechanical Properties of High-Strength Concrete", Journal of Materials in Civil Engineering, 14, 230-238, 2002.

Saadatmanesh, H. and Ehsani, M., "RC beams Strengthened with GFRP Plates. I: Experimental study", ASCE Journal of Structural Engineering, 117, 3417-3433, 1991.

Spadea, G., Bencardino, F. and Swamy, R.N., "Structural Behaviour of Composite RC Beams with Externally Bonded CFRP", Journal of Composites for Construction, 2, 132-137, 1998.

Spadea, G., Swamy, R.N. and Bencardino, F., "Strength and Ductility of RC Beams Repaired with Bonded CFRP Laminates", Journal of Bridge Engineering, 6, 349-55, 2001.

Teng, J.G., Chen, J.F., Smith, S.T. and Lam, L., FRP Strengthened RC Structures, Wiley. New York, 2002.

Thomsen, H.H., Spacone, E., Limkatanyu, S. and Camata, G. "Failure Mode Analysis of Reinforced Concrete Beams Strengthened in Flexure with Externally Bonded Fibre- Reinforced Polymers", Journal of Composites for Construction, 8, 123-131, 2004.

Toutanji, H., Zhao, L. and Zhang, Y., "Flexural Behaviour of Reinforced Concrete Beams Externally Strengthened with CFRP Sheets Bonded with an Inorganic Matrix", Engineering Structures, 28, 557-566, 2006.

Wang, Y.C. and Hsu, K., "Design Recommendations for the Strengthening of Reinforced Concrete Beams with Externally Bonded Composite Plates." Composite Structures, 2008, (in press).

Xiong, G.J., Jiang, X., Liu, J.W. and Chen, L., "A Way for Preventing Tension Delamination of Concrete Cover in Midspan of FRP Strengthened Beams", Construction and Building Materials, 21, 402-408, 2007.